N-Glycosylation and Conserved Cysteine Residues in RAMP3 Play a Critical Role for the Functional Expression of CRLR/RAMP3 Adrenomedullin Receptor†

Marjorie Flahaut, Corinne Pfister, Bernard C. Rossier, and Dmitri Firsov*

Institut de Pharmacologie et de Toxicologie, Université de Lausanne, CH-1005 Lausanne, Switzerland

Received May 8, 2003; Revised Manuscript Received July 10, 2003

ABSTRACT: The calcitonin receptor-like receptor (CRLR) and receptor activity modifying protein-3 (RAMP3) can assemble into a CRLR/RAMP3 heterodimeric receptor that exhibits the characteristics of a high affinity adrenomedullin receptor. RAMP3 participates in adrenomedullin (AM) binding via its extracellular N-terminus characterized by the presence of six highly conserved cysteine residues and four N-glycosylation consensus sites. Here, we assessed the usage of these conserved residues in cotranslational modifications of RAMP3 and addressed their role in functional expression of the CRLR/RAMP3 receptor. Using a *Xenopus* oocyte expression system, we show that (i) RAMP3 is assembled with CRLR as a multiple N-glycosylated species in which two, three, or four consensus sites are used; (ii) elimination of all *N*-glycans in RAMP3 results in a significant inhibition of receptor [^{125}I]AM binding and an increase in the EC_{50} value for AM; (iii) several lines of indirect evidence indicate that each of the six cysteines is involved in disulfide bond formation; (iv) when all cysteines are mutated to serines, RAMP3 is N-glycosylated at all four consensus sites, suggesting that disulfide bond formation inhibits N-gylcosylation; and (v) elimination of all cysteines abolishes adrenomedullin binding and leads to a complete loss of receptor function. Our data demonstrate that cotranslational modifications of RAMP3 play a critical role in the function of the CRLR/RAMP3 adrenomedullin receptor.

Adrenomedullin (AM)[1] and calcitonin gene-related peptide (CGRP) belong to the family of calcitonin-related active peptides that also includes calcitonin and amylin. In 1998, McLatchie et al. have demonstrated that specific receptors to AM and CGRP are formed upon heterodimerization of the calcitonin receptor-like receptor (CRLR), a G protein-coupled receptor, and the receptor activity modifying proteins (RAMPs) (*1*). The RAMP gene family is composed of three members (RAMP1, RAMP2, and RAMP3) that share a low degree of amino acid homology (∼30%) but a common predicted membrane topology with a short cytoplasmic C-terminus, one transmembrane domain, and a large extracellular N-terminus. The CRLR/RAMP1 heterodimer is a specific receptor to CGRP, whereas the CRLR/RAMP2 and CRLR/RAMP3 heterodimers exhibit a high affinity to AM. Mouse CRLR and mouse RAMP3 compose CRLR/RAMP3 heterodimers that also exhibit a high affinity to CGRP (*2*). RAMPs are thus responsible for defining affinity to the ligands of the CRLR.

Structure−function studies have indicated that RAMPs extracellular N-termini play a crucial role in the acquisition of the RAMP-specific receptor phenotypes by CRLR/RAMP heterodimers. Fraser et al., using the construction of chimeric RAMP1/RAMP2 proteins, have demonstrated that only chimeras containing the N-terminal part of RAMP1 were capable of CGRP binding, whereas the N-terminal part of RAMP2 was required for AM binding (*3*). Kuwasako et al. have further identified stretches of seven amino acids in the N-terminal parts of RAMP2 and RAMP3 that are critical for AM binding (*4*, *5*). The N-terminal parts of RAMPs are poorly conserved (less than 20% of amino acid identity) but share in common a significant number of consensus sites for cotranslation modifications including cysteine residues, potentially involved in disulfide bond formation and N-glycosylation consensus sites (Asn-X-Ser/Thr). Sequence alignment of three known mammalian RAMPs (mouse, rat, and human) reveals a similar distribution of cysteine residues in the N-termini of RAMP1, RAMP2, and RAMP3, where four cysteines are conserved in all three RAMPs and two additional cysteines are conserved between RAMP1 and RAMP3. In contrast, consensus sites for N-glycosylation are distributed in a RAMP-specific manner: for RAMP1 there is no N-glycosylation consensus site in any of the three species, whereas one to four consensus sites are present in the N-termini of RAMP2 and RAMP3 sequences. For RAMP3, four consensus sites for N-glycosylation are present and conserved among the three species. For RAMP2, four, three, and one consensus N-glycosylation sites are present in mouse, rat, and human sequences, respectively (reviewed in refs *6* and *7*). In a recent study, we have demonstrated that N-glycosylated RAMP2 and RAMP3 are expressed at the cell surface, and their transport to the plasma membrane

† This work was supported by a Swiss National Fund for Scientific Research, Grants 3100-065140.01/1 (to D.F.) and 3100-061966.00/1 (to B.C.R.), and by the Novartis Foundation.

* To whom correspondence should be addressed. Phone: (41)-(21)-692-5406. Fax: (41)-(21)-692-5355. E-mail: dmitri.firsov@ipharm.unil.ch.

[1] Abbreviations: CRLR, calcitonin receptor-like receptor; RAMP, receptor activity modifying protein; AM, adrenomedullin; CGRP, calcitonin gene-related peptide; Endo H, endoglycosidase H; PNGase F, *N*-glycosidase F; CFTR, cystic fibrosis transmembrane regulator.

10.1021/bi0347508 CCC: $25.00
Published on Web 08/08/2003

requires N-glycans, whereas RAMP1 is not N-glycosylated and is transported to the cell surface only upon formation of heterodimers with CRLR (*8*). In the same study, the coexpression of CRLR with RAMP1 and N-glycosylation mutants of RAMP2 and RAMP3 have revealed that RAMPs are not required for CRLR trafficking to the cell surface but rather involved in the formation of the receptor binding pocket.

It is not known, however, which of these conserved sites are actually utilized in RAMPs cotranslational modifications and what their contribution is in the formation of a functional CRLR/RAMP receptor. Here, we addressed this question by systematically mutating conserved cysteine residues and asparagines in the N-glycosylation consensus site of RAMP3. We selected RAMP3 for the present study since its N-glycosylation consensus sites and cysteine residues are all conserved among mouse, rat, and human RAMP3 sequences. The wild-type and mutant RAMP3 were expressed alone or with CRLR in the *Xenopus* oocytes expression system, and the usage of the consensus sites was estimated by SDS−PAGE. Cell-surface expression of the mutants was assessed, using a highly sensitive binding assay allowing quantitative detection of RAMPs and CRLR at the cell surface, independently of ligand binding. Functional consequences of elimination of these consensus sites were estimated by measurement the EC_{50} value of AM to the CRLR/RAMP3 receptor. AM affinity to CRLR/RAMP3 was determined using a radioligand binding assay that was specially designed for the *Xenopus* oocytes expression system. Our data suggest that (i) RAMP3 is assembled with CRLR as a multiple N-glycosylated species in which two, three, or four consensus sites are used; (ii) the inefficient use of two consensus sites (Asn^{28} and Asn^{57}) is responsible for the expression of multiple N-glycosylated RAMP3 species; (iii) the usage of Asn^{28} and Asn^{57} is hindered by disulfide bond formation; (iv) several lines of indirect evidence indicate that each of the six cysteines is involved in disulfide bond formation; and (v) conserved cysteines are required, and *N*-glycans play an important role in CRLR/RAMP3 receptor function.

EXPERIMENTAL PROCEDURES

cDNA Constructs, FLAG Epitope Insertion, and Site-Directed Mutagenesis. Mouse cDNAs for RAMP3 and CRLR were used in this study. The corresponding proteins were tagged with the FLAG reporter octapeptide DYKDDDDK, as described (*8*). RAMP3 Asn28Ser, Asn57Ser, Asn70Ser, Asn102Ser, Cys27Ser, Cys39Ser, Cys56Ser, Cys71Ser, Cys81Ser, and Cys103Ser mutants were prepared by site-directed mutagenesis, using a PCR based approach. All tagged constructions and mutants were confirmed by cDNA sequencing.

CRLR and RAMP3 Expression in Xenopus Oocytes. Complementary RNAs for CRLR and RAMP3 were synthesized in vitro, using SP6 polymerase. Equal amounts of wild-type or mutant CRLR and RAMP3 cRNA were injected into *Xenopus* oocytes (10 ng of total cRNA/oocyte). Injected oocytes were kept into modified Barth solution (MBS) containing 88 mM NaCl, 1 mM KCl, 2.4 mM $NaHCO_3$, 0.8 mM $MgSO_4$, 0.3 mM $Ca(NO_3)_2$, 0.4 mM $CaCl_2$, and 10 mM Hepes-NaOH (pH 7.2).

Cell-Surface Binding Analysis of RAMP3 Wild-Type and Mutant Proteins in Xenopus Oocytes. Cell-surface expression of wild-type and mutant RAMP3 was quantitatively determined by specific binding of $[^{125}I]M_2IgG_1$ iodinated anti-FLAG M_2 antibody (^{125}I-M_2Ab). M_2Ab was iodinated using the Iodo-Beads iodination reagent (Pierce) and carrier-free $Na^{125}I$ (Hartmann), according to the Pierce protocol. The iodinated antibody had a specific activity of $2-10 \times 10^{17}$ cpm/mol. Binding of the iodinated antibody to oocytes expressing the FLAG-tagged wild-type or mutant RAMP3 with or without CRLR was determined 24−48 h after cRNA injection, as described (*8*). Specific binding was calculated as the difference of the binding between the oocytes injected with FLAG-tagged cRNAs and the noninjected oocytes. Typically, the specific binding was ∼1000 cpm/oocyte, and the nonspecific binding on noninjected oocytes was ∼100 cpm/oocyte.

Radioligand Binding Assay in Xenopus Oocytes Expression System. Rat AM (*1*−*50*) was iodinated using the Iodo-Beads iodination reagent (Pierce) and carrier-free $Na^{125}I$ (Hartmann), according to the Pierce protocol. Briefly, the reaction was initiated in a 2 mL Eppendorf tube in which one Iodo-Bead was placed in the mixture of 85 μL of 0.1 M phosphate buffer (pH 6.5) and 500 μCi (5 μL) of $Na^{125}I$. After 10 min of incubation, 10 μg (10 μL) of rat Adrenomedullin (Calbiochem) was added, and the reaction was continued for an additional 10 min. Unincorporated ^{125}I was removed from the iodinated AM by gel filtration on a PD-10 column (Pharmacia). The iodinated AM was collected into 500 μL of MBS fractions. Fractions seven, eight, and nine containing ^{125}I-AM were pooled, and the quantity of ^{125}I incorporated into AM was determined by TCA precipitation. Iodinated AM had a specific activity of $(1-3) \times 10^{16}$ cpm/mol.

The dissociation constant (K_d) of ^{125}I-AM to the CRLR/RAMP3 receptor was determined on the oocytes injected with cRNAs encoding CRLR and FLAG-tagged wild-type or mutant RAMP3. Forty-eight h after injection, 12 oocytes were transferred into a 2 mL Eppendorf tube containing 100 μL of binding buffer (MBS supplemented with 1% BSA). After 30 min of incubation on ice, the binding buffer was replaced by 100 μL of ice-cold binding buffer containing ^{125}I-AM (5×10^{-7} to 10^{-9} M). After 1 h of incubation on ice, the oocytes were washed six times with 1 mL of ice-cold binding buffer and then transferred individually into tubes for γ counting. Nonspecific binding was determined on the oocytes injected with the same cRNA mixture using the ^{125}I-AM-containing binding buffer supplemented with 10^{-5} Mnonradioactive AM. In a typical assay, the specific binding signal at saturating concentrations of AM (10^{-7} M) was ∼500 cpm/oocyte, and the nonspecific binding was ∼200 cpm/oocyte.

Oocytes [^{35}S]methionine Metabolic Labeling and Protein Immunoprecipitation. Endoglycosidase H (Endo H) and N-Glycosidase F (PNGase F) Treatment of Immunoprecipitates. Oocytes were injected with wild-type or mutant RAMP3 with or without CRLR and incubated overnight in MBS containing 0.8 mCi/mL [^{35}S]methionine (NEN). Microsomes were prepared as described (*9*), and microsomal proteins were solubilized in a digitonin washing buffer (DWB) containing 20 mM Tris pH 7.6, 100 mM NaCl, 0.5% digitonin, 1 mM phenylmethylsulfonyl fuoride (PMSF), and 5 μg/mL of each leupeptin, antipain, and pepstatin A. Immunoprecipitation was performed overnight with an anti-RAMP3 polyclonal antibody or with an M2 anti-FLAG

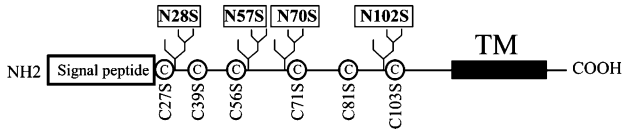

FIGURE 1: Linear model of RAMP3. This model shows the N-terminal signal peptide domain, the C-terminal transmembrane domain (TM), six cysteine residues, and four N-glycosylation consensus sites located in the extracellular part of RAMP3. The amino acid sequence numbers of these residues as well as their replacements are indicated.

monoclonal antibody at 4 °C. The immunoprecipitates were recovered with protein A-Agarose beads (for the anti-RAMP3 polyclonal antibody) or with protein G-Sepharose beads (for the M2 anti-FLAG monoclonal antibody)and washed six times with DWB and one time with DWB not containing digitonin. Samples assigned for Endo H or PNGase F treatments were additionally washed one time with the respective enzyme buffers, and Endo H or PNGase F treatments were performed overnight (37 °C) in a 100 μL reaction mixture containing immunoprecipitate/beads complexes and 10 units of Endo H or PNGase F (New England Biolabs) in the respective enzyme buffer. The immunoprecipitates were resolved by an 8−13% gradient SDS−PAGE and revealed by fluorography. For nonreducing conditions, the β-mercapthoethanol was removed from the sample buffer.

RAMP3 Rabbit Polyclonal Antibody. Rabbit anti-RAMP3 polyclonal antibody was prepared, using a glutathion-transferase (GST)-fusion protein that encompasses the amino acids Cys^{27}−Met^{47} in the N-terminal part of the mouse RAMP3. This antibody was revealed as highly specific for immunoprecipitation of RAMP3 but was inefficient in the Western blot and cellular immunostaining applications.

Determination of EC_{50} Values of CRLR/RAMP3 Receptor in the Xenopus Oocytes. CRLR and wild-type or mutant RAMP3 cRNAs were coinjected into *Xenopus* oocytes, together with cRNA encoding for the cystic fibrosis transmembrane regulator (CFTR), a cAMP-activated chloride channel. Injected oocytes were kept into MBS for 20 h. The EC_{50} values were determined by measurements of AM-generated Cl^- currents generated by CFTR, according to Chraibi et al. (*10*). The current was measured under a two-electrode voltage clamp at a potential oscillating between −40 and −80 mV. The chloride conductance was then calculated.

RESULTS

RAMP3 Expression Pattern in Xenopus Laevis Oocytes. Signal peptide-processed RAMP3 contains four N-glycosylation consensus sites and six cysteine residues highly conserved across the mouse, rat, and human RAMP3 amino acid sequences (Figure 1). To assess the usage of these conserved residues in cotranslational modifications of RAMP3, we characterized the protein expression pattern of mouse RAMP3 in the *X. laevis* oocytes expression system. Oocytes were injected with RAMP3 cRNA and metabolically labeled with [^{35}S]methionine, and RAMP3 protein was immunoprecipitated with an anti-RAMP3 antibody. As shown in Figure 2A (lane 1), RAMP3 is expressed as three molecular species with apparent molecular weights (*Mr*) of 20, 23, and 26 kDa. The relative abundance of these three RAMP3 species was not changed upon different chase periods lasting up to 48 h

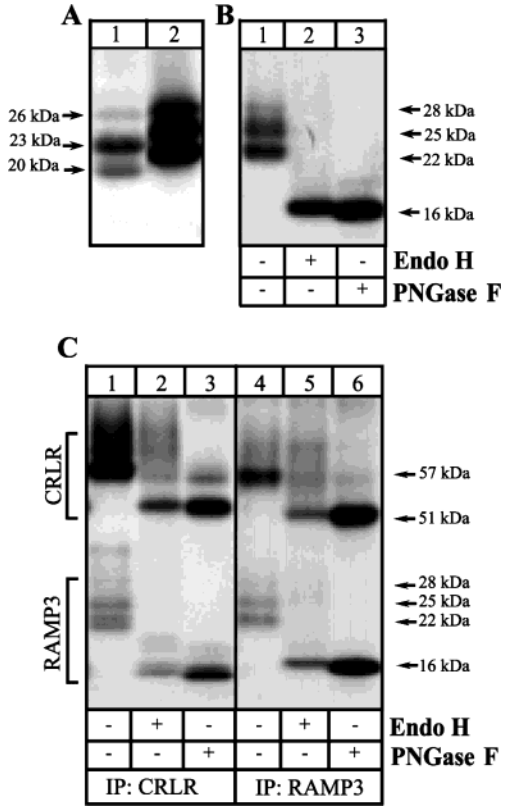

FIGURE 2: RAMP3 expression pattern in the *X. laevis* oocytes. (A)-Comparison of untagged and FLAG-tagged RAMP3 expression patterns. Lane 1: oocytes were injected with 3 ng/oocyte of untagged RAMP3 cRNA, [^{35}S]methionine was metabolically labeled (overnight), and untagged RAMP3 was immunoprecipitated with an anti-RAMP3 antibody. Lane 2: oocytes were injected with 3 ng/oocyte of FLAG-tagged RAMP3 cRNA, [^{35}S]methionine was metabolically labeled (overnight), and FLAG-tagged RAMP3 was immunoprecipitated M2 anti-FLAG monoclonal antibody. The immunoprecipitated RAMP3 was separated on 8−13% gradient SDS−PAGE. (B) Sensitivity of immunoprecipitated RAMP3 to Endo H or PNGase F treatments. FLAG-tagged RAMP3 was expressed in the oocytes. Oocytes were [^{35}S]methionine metabolically labeled, and RAMP3 was immunoprecipitated, using the M2 anti-FLAG antibody. The immunoprecipitated product was divided into three parts: one of them was subjected to Endo H treatment (lane 2), the second one was subjected to PNGase F treatment (lane 3), and the third one was treated in a similar way as the PNGase F-treated part but without enzyme addition (lane 1). (C) Cross-immunoprecipitation of CRLR/RAMP3 complexes. Oocytes were injected with mix of FLAG-tagged CRLR cRNA and untagged RAMP3 cRNA (3 ng of each cRNA/oocyte) or with a mix of untagged CRLR and FLAG-tagged cRNAs (3 ng of each cRNA/oocyte), and [^{35}S]methionine was metabolically labeled (overnight). Immunoprecipitation was performed under nondenaturing conditions, using M2 anti-FLAG antibody. In lanes 1−3, untagged RAMP3 was coimmunoprecipitated with FLAG-tagged CRLR. The immunoprecipitated product was either subjected to Endo H treatment (lane 2), to PNGase F treatment (lane 3), or was treated in a similar way as the PNGase F-treated part but without enzyme addition (lane 1). In lanes 4−6, untagged CRLR was coimmunoprecipitated with FLAG-tagged RAMP3. The immunoprecipitated product was either subjected to Endo H treatment (lane 5), to PNGase F treatment (lane 6), or was treated in a similar way as the PNGase F-treated part but without enzyme addition (lane 4).

(data not shown). The FLAG-tagged RAMP3, which was further used in this study, shows a similar three-band pattern (22, 25, and 28 kDa species) that was shifted to the higher apparent *Mr* (shift ∼2 kDa) because of the presence of the FLAG epitope (Figure 2A, lane 2).

Expression of multiple RAMP3 molecular species most likely reflects the difference in the degree of N-linked glycosylation in these RAMP3 species. The N-glycosylation of glycoproteins starts with the addition in the ER of high mannose core sugars to the nascent polypeptide chain from dolichol precursors. The core sugars are then trimmed during the transport of the polypeptide to the Golgi, and finally complex-type sugars such as galactose or sialic acid are added in a trans-Golgi compartment (terminal or fully glycosylation). However, this mechanism does not automatically ensure N-glycosylation, as many proteins containing the Asn-X-Ser/Thr consensus site remain either nonglycosylated or glycosylated to a variable extent. Thus, the multiple molecular species of RAMP3 most likely result from either the formation of different core-glycosylated forms of RAMP3 or from the formation of a mixture of core- and fully glycosylated RAMP3 species. To distinguish between these two possibilities, we treated the immunoprecipitated RAMP3 either with endoglycosidase H (Endo H) that cleaves the chitobiose of the high mannose core sugars or with *N*-glycosidase F (PNGase F) that removes all types of N-linked sugars (core and complex type glycans). As shown in Figure 2B, the treatment with both Endo H (lane 2) and PNGase F (lane 3) leads to the decrease in the apparent *Mr* of all three RAMP3 species to a single protein species with an apparent *Mr* of ~16 kDa, corresponding to the theoretical apparent *Mr* for nonglycosylated RAMP3. The small difference (~0.5 kDa) in the apparent *Mr* observed between Endo H and PNGaseF treated RAMP3 is probably explained by the presence of uncleaved *N*-acetylglucosamine in the Endo H-treated samples. These experiments show that when expressed alone, RAMP3 is present in multiple core-glycosylated species. Since the occupancy of a single N-glycosylation consensus site by the high mannose sugars is responsible for an increase in the apparent *Mr* of ~3 kDa, it indicates that a 22, 25, and 28 kDa molecular species of FLAG-tagged RAMP3 represents the RAMP3 protein with two, three, and four N-glycosylation consensus sites used, respectively. Thus, these data also indicate that RAMP3 can be N-glycosylated on all four consensus sites, albeit highly inefficiently.

To check whether the heterogeneous RAMP3 expression pattern is also characteristic for RAMP3 assembled with CRLR, we coexpressed CRLR and RAMP3 in *Xenopus* oocytes and performed a nondenaturing coimmunoprecipitation of CRLR/RAMP3 heterodimers with an anti-FLAG antibody directed against the FLAG epitope inserted either in CRLR or in RAMP3. As shown in Figure 2C, a similar RAMP3 expression pattern was observed whether the FLAG epitope was present in CRLR (Figure 2C, lane 1) or in RAMP3 (Figure 2C, lane 4). In both cases, all RAMP3 species could be reduced by Endo H (lanes 2 and 5) or PNGase F (lanes 3 and 6) treatment to the single bands with an apparent *Mr* of ~14 and ~16 kDa, for untagged and FLAG-tagged RAMP3, respectively. Trace amounts of an additional protein product (*Mr* ~19 kDa) visible in lane 2 (Endo H treatment) are also present in lane 3 (PNGaseF treatment) but shifted by ~1−2 kDa to a lower molecular weight. Therefore, this band represents either partially deglycosylated RAMP3 or a degradation product of CRLR. CRLR was expressed as a major core-glycosylated species with an apparent *Mr* of ~57 kDa that could be reduced by Endo H or PNGase F treatments to the nonglycosylated species with an apparent *Mr* of ~51 kDa. A minor Endo H-resistant form for CRLR was detected as a smear with an apparent *Mr* of ~60−65 kDa. Altogether, these experiments show that RAMP3 is assembled with CRLR in multiple core-glycosylated species.

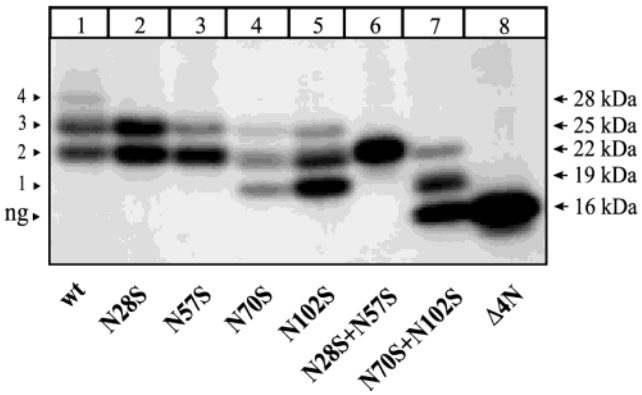

FIGURE 3: Characterization of RAMP3 N-glycosylation pattern. Asparagine residues in the N-glycosylation consensus sites of RAMP3 were replaced with serines, and wild-type or mutant RAMP3 was expressed in oocytes. After [^{35}S]methionine metabolic labeling (overnight), the wild-type and mutant RAMP3 was immunoprecipitated with M2 anti-FLAG antibody. Immunoprecipitated protein was separated on an 8−13% gradient SDS−PAGE.

Mutational Analysis of RAMP3 Putative N-Glycosylation Sites. To assess the usage and the functional roles of individual RAMP3 N-glycosylation consensus sites, we prepared mutants in which the asparagine residues were replaced by serines (N28S, N57S, N70S, and N102S). The wild-type and mutant RAMP3 were expressed in *Xenopus* oocytes and immunoprecipitated under denaturing conditions. Analysis of single mutants reveals the disappearance of ~28 kDa for the four mutants (Figure 3, lanes 2−5) and the appearance of an additional band of ~19 kDa for N70S and N102S mutants but not for N28S and N57S mutants (Figure 3, lanes 4 and 5). This ~19 kDa band most likely corresponds to the RAMP3 protein with a single N-glycosylation site used. The appearance of a RAMP3 species glycosylated on a single site in N70S and N102S mutants but not in N28S and N57S mutants indicated that Asn^{70} and Asn^{102} are glycosylated more efficiently than Asn^{28} and Asn^{57}. Analysis of immunoprecipitation patterns of double mutants (Figure 3, lanes 6 and 7) confirms that the N28S-N57S mutant is efficiently glycosylated on two remaining sites, whereas the N70S-N102S mutant was predominantly present in the nonglycosylated form. The apparent *Mr* of the RAMP3-Δ4N quadruple mutant (16 kDa) corresponded to the apparent *Mr* of nonglycosylated RAMP3 (Figure 3, lane 8). Collectively, these results demonstrate that the inefficient use of two consensus sites (Asn^{28} and Asn^{57}) is mostly responsible for the expression of multiple N-glycosylated RAMP3 species.

Functional and Cell-Surface Expression of RAMP3 N-Glycosylation Mutants. To assess the role of RAMP3 N-glycosylation in the functional expression of the CRLR/RAMP3 receptor, we took advantage of its coupling to cAMP production. We measured the dose-dependency of AM-stimulated currents generated by CFTR, a cAMP-activated chloride channel. CFTR, CRLR, and RAMP3 cRNAs were coinjected in oocytes, and the effector concentrations for a half-maximal response (EC_{50}) for AM were determined. As

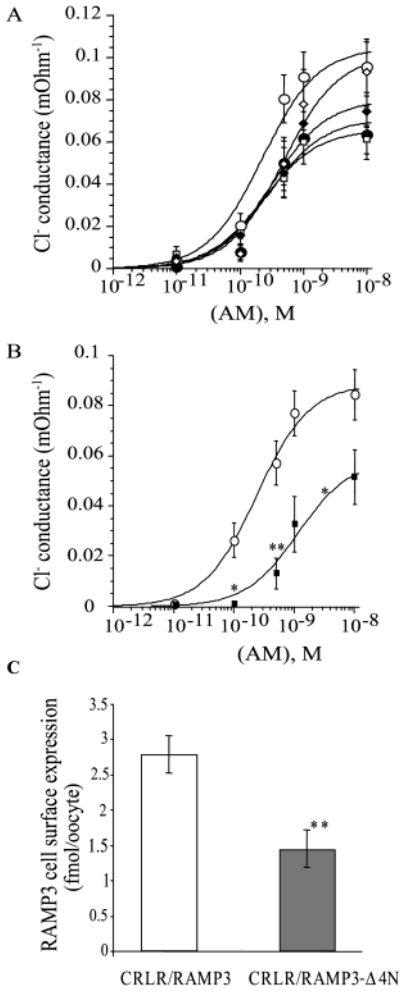

FIGURE 4: RAMP3 N-glycosylation is important for expression of the fully functional CRLR/RAMP3 receptor. (A) The EC_{50} value for AM was determined by measurement of AM-generated Cl^- currents in the oocytes coinjected with CFTR, CRLR, and wild-type (○) or N28S (●), N57S (□), N70S (◆), and N102S (◇) mutant RAMP3. (B) The same experiment was performed with RAMP3-Δ4N mutant (■). (C) Oocytes were injected with CRLR and FLAG-tagged wild-type or mutant RAMP3. RAMP3 cell-surface expression was determined by the binding of ^{125}I-labeled M2 anti-FLAG antibody. Error bars are mean ± SE of the experiment performed with 12 oocytes per experimental condition; ** denotes statistical significance <0.005.

shown in Figure 4A, the N70S and N102S mutations caused a shift in the EC_{50} value to the right as compared to the wild-type CRLR/RAMP3 receptor, but only for the N102S mutant did this shift reach the statistical significance (CRLR/RAMP3wt: $EC_{50} = 228 \pm 41$ pM, $n = 6$; CRLR/RAMP3-N102S: $EC_{50} = 582 \pm 109$ pM, $n = 5$, $p < 0.05$). The EC_{50} values for the N28S and N57S mutants were not significantly different from the wild-type receptor. The individual N-glycosylation mutant of RAMP3 was expressed at the cell surface at the intermediate levels between the CRLR/RAMP3 and the CRLR/RAMP3-Δ4N mutant (data not shown). In a second series of experiments, mutations of all four consensus sites (RAMP3-Δ4N mutants) led to an over 6-fold increase in the EC_{50} value for AM (CRLR/RAMP3wt: $EC_{50} = 296 \pm 48$ pM, $n = 13$; CRLR/RAMP3-Δ4N: $EC_{50} = 1905 \pm 533$ pM, $n = 11$, $p < 0.005$) (Figure 4B). Importantly, the mutation of all four consensus sites also resulted in a lower cell-surface expression of the

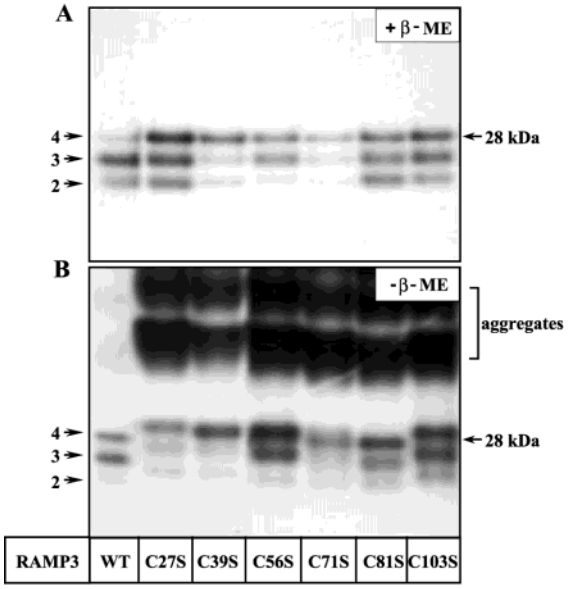

FIGURE 5: Effects of cysteine to serine substitutions on RAMP3 N-glycosylation and gel mobility under nonreducing conditions. Conserved cysteine residues in RAMP3 were replaced by serines, and cRNAs (3 ng/oocyte) for wild-type or mutant RAMP3 were injected in *Xenopus* oocytes. Oocytes were [^{35}S]methionine metabolically labeled (overnight), and wild-type or mutant RAMP3 were immunoprecipitated, using M2 anti-FLAG antibody. Immunoprecipitated product was divided in two equal samples: (A) in the first sample, the immunoprecipitated product was recovered from the protein G-beads using sample buffer containing *β*-mercaptoethanol (reducing condition). (B) in the second sample, the immunoprecipitated product was recovered from the protein G-beads using sample buffer not containing *β*-mercaptoethanol (nonreducing condition). Immunoprecipitated proteins were separated on an 8−13% gradient.

RAMP3-Δ4N mutant as compared to RAMP3wt, when coexpressed with CRLR (Figure 4C).

Interactions between N-Glycosylation and Disulfide Bond Formation in RAMP3. The low efficiency of N-glycosylation on the Asn^{28} and Asn^{57} residues suggested that some molecular determinants intrinsic to the RAMP3 sequence may impair the attachment of N-linked sugars to these sites. Two major causes of the inefficient use of the N-glycosylation consensus sites have been described. First, a proline residue in the X position of the Asn-X-Ser/Thr consensus sites has been shown to impair N-glycosylation (*11*). Second, the formation of disulfide bonds and the subsequent rapid folding of the nascent polypeptide chain may block the access of oligosacharyl transferase to the addition site from the ER lumen (*12*−*14*). Analysis of the RAMP3 amino acid sequence revealed no proline residues in the Asn^{28} and Asn^{57} consensus sites making the second mechanism the most plausible. To check whether the conserved cysteine residues might be the factor preventing N-glycosylation of RAMP3, we replaced all cysteines by serines and expressed these mutants in *Xenopus* oocytes. As shown in Figure 5A, the mutation of single cysteine residues results in a significant increase in the relative abundance of the RAMP3 species with four N-glycosylation sites used. Using densitometry analysis, we estimated the relative abundance of this species as compared to the total amount of immunoprecipitated RAMP3. For the experiment presented in Figure 5, the relative abundance of RAMP3 with four N-glycosylation sites used increases from ∼15% for the wild-type RAMP3 up to

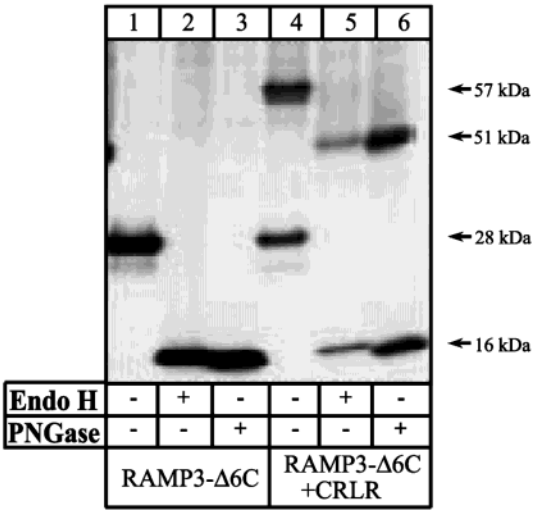

FIGURE 6: RAMP3-Δ6C mutant is expressed as a molecular species in which all the four N-glycosylation consensus sites are used. Oocytes were injected either with RAMP3-Δ6C (FLAG-tagged) cRNA alone (lanes 1−3) or in combination with nontagged CRLR (lanes 4−6). Immunoprecipitation was performed under nondenaturing conditions, using M2 anti-FLAG antibody. Immunoprecipitated proteins were subjected or not subjected to either Endo H (lanes 2 and 5) or PNGase F treatment (lanes 3 and 6).

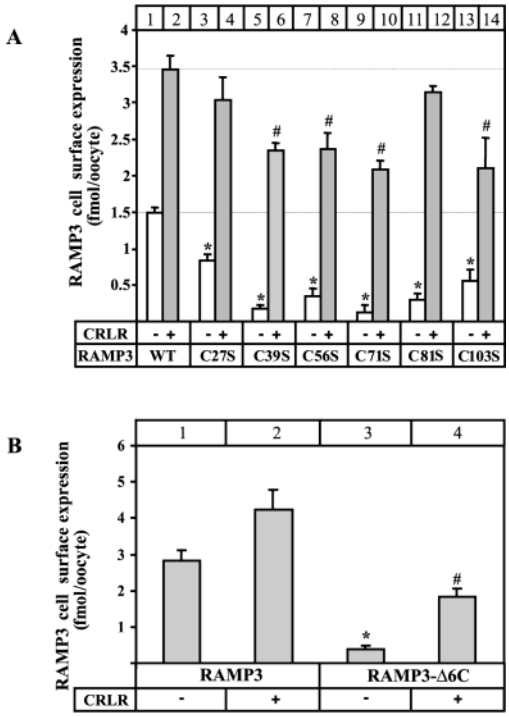

FIGURE 7: Effect of cysteine to serine mutations on RAMP3 cell-surface expression. (A) Oocytes were injected with FLAG-tagged individual cysteine mutants of RAMP3 alone or in combination with CRLR. RAMP3 cell-surface expression was determined by the binding of ^{125}I-labeled M2 anti-FLAG antibody. Error bars are mean ± SE of three experiments performed with 12 oocytes per experimental condition, * denotes statistical significance <0.001 between cell-surface expression of wild-type and cysteine mutants expressed alone, and # denotes statistical significance <0.005 between cell-surface expression of wild-type and cysteine mutants coexpressed with CRLR. (B) The same experiment was performed with the RAMP3-Δ6C mutant.

∼40% for the C27S mutant, ∼56% for the C39S mutant, ∼43% for the C56S mutant, ∼47% for the C71S mutant, ∼33% for the C81S mutant, and ∼40% for the C103S mutant. Two additional independent experiments have confirmed this observation (data not shown). SDS−PAGE separation of the same immunoprecipitated material under nonreducing conditions (Figure 5B) shows that four out of six cysteine mutants (C27S, C39S, C56S, and C103S) have a significantly reduced gel mobility as compared to the wild-type RAMP3. All single cysteine mutants, but not wild-type RAMP3, were capable of the formation of multimeric aggregates of higher molecular weights (Figure 5B). The formation of the aggregates was observed in four independent experiments; however, their molecular identity remains unclear.

Altogether, these results indicate that the conserved cysteine residues are involved in disulfide bond formation and that the formation of disulfide bonds impedes efficient glycosylation of RAMP3. To provide an additional support for the latter hypothesis, we also prepared a FLAG-tagged mutant in which the six cysteine residues were replaced by serines (RAMP3-Δ6C mutant). As shown in Figure 6, the RAMP3-Δ6C mutant is expressed as a single molecular species with an apparent *Mr* of ∼28 kDa (lane 1). The treatment of the immunoprecipitated product with either Endo H or PNGase F reduced this band to a single molecular species with an apparent *Mr* of ∼16 kDa (Figure 6, lanes 2 and 3), thus indicating that a 28 kDa species of RAMP3-Δ6C corresponds to the RAMP3 protein with all four N-glycosylation sites used. Strikingly, coexpression and coimmunoprecipitation of the FLAG-tagged RAMP3-Δ6C mutant with the nontagged CRLR showed that this mutant was still capable of association with CRLR and that its glycosylation pattern was not different from that of the RAMP3-Δ6C mutant expressed alone (Figure 6, lanes 4−6). The 57 and 51 kDa species in lanes 4−6 correspond to the glycosylated (lane 4) and nonglycosylated (lanes 5 and 6) forms of CRLR.

Cell-Surface Expression of RAMP3 Cysteine Mutants. To check whether the elimination of cysteine residues affects the routing to the cell surface of RAMP3, we measured the cell-surface expression level of RAMP3 cysteine mutants expressed either alone or in combination with CRLR. As shown in Figure 7A, the mutation of any of the cysteine residues leads to a significant decrease in the RAMP3 cell-surface expression as compared to the wild-type RAMP3 (open bars) [RAMP3 wt (lane 1): 1.50 ± 0.06 fmol/oocyte, $n = 29$; RAMP3 C27S (lane 3): 0.83 ± 0.01 fmol/oocyte, $n = 36$, $p < 0.001$; RAMP3 C39S (lane 5): 0.18 ± 0.04 fmol/oocyte, $n = 36$, $p < 0.001$; RAMP3 C56S (lane 7): 0.34 ± 0.11 fmol/oocyte, $n = 36$, $p < 0.001$; RAMP3 C71S (lane 9): 0.13 ± 0.09 fmol/oocyte, $n = 36$, $p < 0.001$; RAMP3 C81S (lane 11): 0.29 ± 0.10 fmol/oocyte, $n = 35$, $p < 0.001$; and RAMP3 C103S (lane 13): 0.56 ± 0.16 fmol/oocyte, $n = 36$, $p < 0.001$]. Coexpression of these mutants with CRLR (dashed bars) dramatically increased the cell-surface expression of all mutants: the cell-surface expression of the C27S (lane 4) and C81S (lane 12) mutants was identical to the wild-type RAMP3 coexpressed with CRLR, whereas cell-surface expression of C39S (lane 6), C56S (lane 8), C71S (lane 10), and C103S (lane 14) mutants was lower

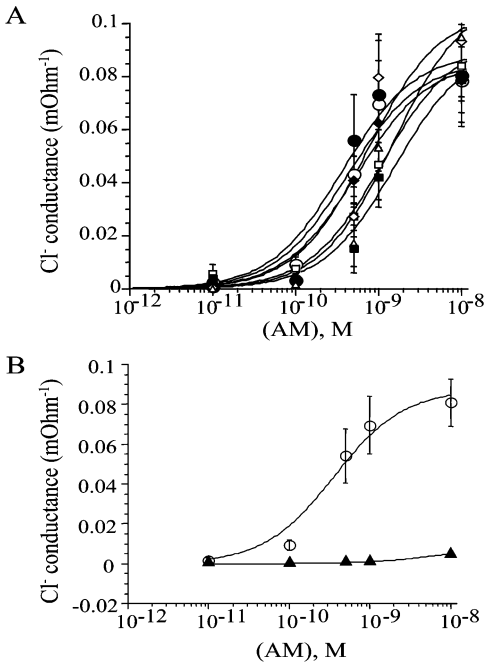

FIGURE 8: Conserved cysteine residues are required for expression of the fully functional CRLR/RAMP3 receptor. (A) The EC_{50} value for AM was determined by measurement of AM-generated Cl^- currents in the oocytes coinjected with CFTR, CRLR, and wild-type (○) or C27S (●), C39S (□), C56S (◆), C71S (◇), C81S (△), and C103S (■) mutant RAMP3. (B) The same experiment was performed with RAMP3-Δ6C mutant (▲).

than the wild-type receptor but still significantly higher than the mutants expressed without CRLR (Figure 7A). We also tested the effect of elimination of the six cysteine residues (RAMP3-Δ6C mutant) on the cell-surface expression of RAMP3. As shown in Figure 7B, the RAMP3-Δ6C mutant is expressed at the cell surface at a low level (lane 3) as compared with the wild-type RAMP3 (lane 1). Importantly, cell-surface expression of the RAMP3-Δ6C mutant was partially restored upon coexpression with CRLR (lane 2 vs 4).

Conserved Cysteine Residues in RAMP3 Are Required for Formation of Functional CRLR/RAMP3 Receptor. Since the conserved cysteine residues are required for proper N-glycosylation and cell-surface expression of RAMP3, we also examined whether elimination of these residues affects the EC_{50} values to AM of the CRLR/RAMP3 receptor. As shown in Figure 8A, most of the cysteine mutants had the tendency to increase the EC_{50} values to AM as compared to the wild-type CRLR/RAMP3 receptor, but only for the C81S and C103S mutations did this increase reach statistical significance (CRLR/RAMP3wt: $EC_{50} = 627 \pm 191$ pM, $n = 11$; CRLR/RAMP3-C81S: $EC_{50} = 2580 \pm 1118$ pM, $n = 7$, $p < 0.05$; and CRLR/RAMP3-C103S: $EC_{50} = 1829 \pm 578$ pM, $n = 5$, $p < 0.05$). Elimination of the six cysteines (RAMP3-Δ6C mutant) leads to a complete loss of CRLR/RAMP3 receptor function (Figure 8B). Importantly, this loss of function was not due to a lack of CRLR/RAMP3-Δ6C association (Figure 6) or lack of cell-surface expression (Figure 7B) of this receptor.

^{125}I-AM Binding to CRLR/RAMP3wt, RAMP3-Δ4N, and CRLR/RAMP3-Δ6C Receptors. To determine the mechanism of decrease of AM potency to the CRLR/RAMP3-Δ4N receptor and of the loss of function of the CRLR/RAMP3-Δ6C receptor, we developed a binding assay allowing direct measurement of ^{125}I-AM binding sites on the living *Xenopus* oocytes (see Experimental Procedures). Mouse CRLR and mouse wild-type or mutant RAMP3 cRNAs were injected in the oocytes, and ^{125}I-AM binding was measured 48 h after cRNA injection. The apparent dissociation constant (K_d) was measured, using an increasing concentration of ^{125}I-AM, and specific binding was determined as the difference between radioactive labeling of oocytes incubated in the presence or absence of 10^{-5} M of nonradioactive AM. As shown in Figure 9, oocytes expressing the wild-type CRLR/RAMP3 receptor revealed saturable ^{125}I-AM binding with a K_d of 35 ± 6 nM ($n = 20$). No specific binding was detectable on the oocytes injected with water or with the CRLR/RAMP3-Δ6C mutant receptor. Specific binding for the CRLR/RAMP3-Δ4N mutant receptor was detectable only starting from the 2.5×10^{-7} M of AM concentration. These data show that a decrease or loss of binding affinity to the AM of CRLR/RAMP3-Δ4N and CRLR/RAMP3-Δ6C mutants correlates with a decrease or loss of function of these mutants, respectively.

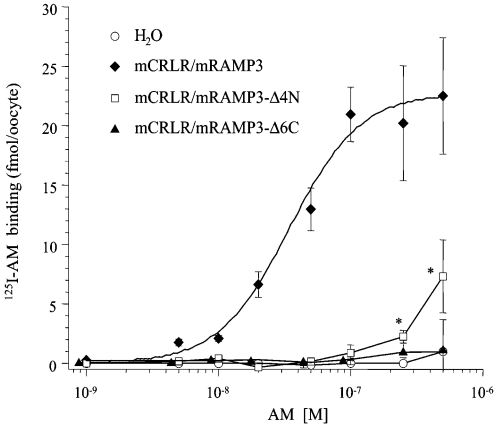

FIGURE 9: AM affinity is decreased or abolished for CRLR/RAMP3-Δ4N and CRLR/RAMP3-Δ6C mutants, respectively. Oocytes were injected either with water (○), or with CRLR/RAMP3 cRNAs (◆), or with CRLR/RAMP3-Δ4N cRNAs (□), or with CRLR/RAMP3-Δ6C cRNAs (▲). ^{125}I-AM binding was determined 48 h after cRNA injection. Error bars are mean ± SE of three experiments performed with 12 oocytes per experimental condition, and * denotes the statistical significance <0.01 in ligand binding between water-injected oocytes and oocytes expressing the CRLR/RAMP3-Δ4N mutant receptor.

DISCUSSION

Most G protein-coupled receptors (GPCR) are cotranslationally modified by N-glycosylation and disulfide bond formation. Disruption of disulfide bonds in GPCRs usually leads to a loss of receptor cell-surface expression and/or ligand binding (*15*−*17*), whereas effects of elimination of *N*-glycans vary from the absence of any known functional consequences to the complete loss of receptor function (*18*−*20*). Among many GPCRs thus far characterized, CRLR remains a unique example of a receptor that requires association with other GPCR-unrelated transmembrane proteins (RAMPs) for formation of its binding pocket. Another receptor, namely, the calcitonin receptor (CTR), is also capable of heterodimerization with RAMPs and the formation of CTR/RAMP1 and CTR/RAMP3 receptors with high affinity to CGRP and amylin, respectively (*21*, *22*). However,

CTR does not require RAMPs for calcitonin binding. Several lines of evidence suggest that in CRLR/RAMP heterodimers the cotranslational modifications of both partners are required for the expression of a fully functional receptor. Buhlmann et al. (*23*) have demonstrated that N-glycosylation is important for receptor cell-surface expression. Kamitani and Sakata (*24*) have identified a role of N-glycosylation in receptor ligand binding and signaling. We have recently demonstrated that the elimination of all N-glycosylation consensus sites in RAMP2 and RAMP3 leads to the complete loss of cell-surface expression of these proteins, whereas the insertion of N-glycosylation consensus sequences in non-glycosylated RAMP1 guides this protein to the cell surface (*8*).

In the *Xenopus* oocyte expression system, RAMP3 is expressed and associated with CRLR as three major molecular species in which two, three, or four N-glycosylation consensus sites are used. All the three species are core-glycosylated as determined by their sensitivity to Endo H. Whether these core-glycosylated RAMP3 species represent the cell-surface expressed RAMP3 remains, however, uncertain. As of today, several examples of cell-surface expressed proteins that remain core-glycosylated on all or some of their N-gylcosylation consensus sites have been described. Of special interest is the case of the amiloride-sensitive sodium channel (ENaC) expressed in the same cell as RAMP3 (*25*−*27*). This phenomenon has also been observed for the nicotinic receptor (*28*) and for the anion exchanger AE1 (*29*) to cite a few among others (*26*, *30*−*33*). Also important in this matter, the N-glycosylation pattern of RAMP3 in the *Xenopus* oocyte expression system is not different from that observed in HEK293 cells (*6*). Recently, Hilairet et al. have attempted the immunoprecipitation of cell-surface expressed RAMP3 in HEK293 cells (*34*). However, in this study the cell-surface expressed RAMP3 could be detected only after EndoH treatment of HEK293 protein extracts, thus leaving open the question of the existence of differentially glycosylated RAMP3 species at the cell surface.

Mutational analysis of individual N-glycosylation consensus sites shows that all of them are used albeit with a variable efficiency: Asn^{70} and Asn^{102} are heavily glycosylated whereas Asn^{28} and Asn^{57} are used highly inefficiently. In search of the cause of the inefficient use of Asn^{28} and Asn^{57} sites, we demonstrated that elimination of all conserved cysteine residues results in the expression of RAMP3 in which all the four asparagines are efficiently N-glycosylated. This suggests that the conserved cysteine residues form disulfide bonds and that disulfide bond formation may inhibit the N-glycosylation of Asn^{28} and Asn^{57}. Additional evidence that cysteines are presumably involved in disulfide bond formation are the following: (i) mutation of individual cysteine residues results in expression of RAMP3 with a significantly higher relative abundance of RAMP3 species in which four N-glycosylation sites are used; (ii) with the exception of C71S and C81S, the SDS−PAGE separation of individual cysteine mutants under nonreducing conditions results in a significantly slower gel mobility, as compared to wild-type RAMP3; and (iii) mutation of each of the six cysteines results in a significant loss of RAMP3 cell-surface expression. Altogether, our data suggest that the six cysteines play an important role in RAMP3 cotranslational folding. During the preparation of this manuscript, a report was published demonstrating that the conserved cysteines in human RAMP2 also play a crucial role in CRLR/RAMP2 receptor function (*35*).

How could the formation of disulfide bonds interfere with the usage of N-glycosylation consensus sites? For most transmembrane and secreted proteins, N-linked oligosaccharides are added cotranslationally. Nilsson and von Heijne (*36*) have demonstrated that the active site of oligosaccharyl transferase is positioned in such a way that the addition site is recognized when 10−11 amino acids have emerged from the translocation pore. Recently, Hasler et al. have shown in a living cell that this distance is shorter by five or six residues (*37*). It has been proposed that disulfide bonds may block oligosaccharide addition if (i) the N-glycosylation consensus site is located in between a disulfide bond-forming cysteine pair and (ii) the distance between the upstream cysteine from the disulfide bond-forming cysteine pair and the N-glycosylation consensus site does not exceed five to six amino acids. If both conditions are present, a disulfide bond could form before the N-glycosylation consensus site emerges enough from the translocation pore and becomes accessible to the oligosaccharyl transferase. Once formed, the disulfide bond could definitely hinder the access for oligosaccharyl transferase. For example, such a mechanism was demonstrated to inhibit the N-glycosylation of hemagglutinin−neuraminidase glycoprotein of the Newcastle disease virus (*13*). The inspection of the RAMP3 amino acid sequence reveals that Asn^{28} and Asn^{57}, but not Asn^{70} and Asn^{102}, could fit such a mechanism (Figure 1). Significantly, this correlates with the usage of the N-glycosylation sites: Asn^{28} and Asn^{57} are used highly inefficiently, whereas Asn^{70} and Asn^{102} are heavily glycosylated. This indicated that the mechanism described above could be one of the possible explanations for the poor glycosylation of Asn^{28} and Asn^{57}. The addition of N-linked sugars to the polypeptide chain can also be limited from the C-terminal side. It has been shown that access of a nascent chain to the oligosaccharyl transferase ends when the nascent chain leaves the ribosome and the translocon (*38*). The distance between the ribosomal translational site (most C-terminal amino acid) and the oligosaccharyl transferase active site was estimated to be in the range of 65 amino acids (*39*). In RAMP3 sequence, Asn^{102} could fit this criteria. This site, however, is efficiently glycosylated. Recent evidence suggested that posttranslational N-glycosylation is also a possible mechanism (*40*−*42*). In some cases, the posttranslational N-glycosylation was proposed to compete with disulfide bond formation (*14*, *42*). In the present study, we did not address whether co- or posttranslational N-glycosylation is responsible for RAMP3 N-glycosylation. Collectively, our data best fit with the mechanism in which the disulfide bond-dependent RAMP3-folding around Asn^{28} and Asn^{57} precedes the N-glycosylation step, thus inhibiting the RAMP3 glycosylation.

For oligomeric transmembrane proteins, the formation of disulfide bonds as well as N-glycosylation are usually critical for assembly and maturation of assembled complexes in the ER compartment (for a review, see ref *43*). For the formation of a CRLR/RAMP3 heterodimer, neither cysteine residues nor *N*-glycans are required (ref *8* and this study). It follows that the RAMP3 transmembrane domain and/or its intracellular C-terminus are sufficient for CRLR-RAMP3 association. As discussed above, none of the RAMP3 N-glyco-

sylated species acquires Endo H-resistance. Therefore, the processing of RAMP3 N-glycosylation sites by Golgi enzymes is probably sterically hindered, most likely as a result of protein folding and/or oligomerization with CRLR. The fact that the RAMP3-Δ6C mutant is also expressed as a core-glycosylated protein suggests that important folding events, other than disulfide bond formation, might be involved.

Functional analysis of mutants of N-glycosylation consensus sites and conserved cysteine residues shows that both types of co(post)translational modifications are required for the expression of a fully functional AM receptor. For N-glycosylation sites, the effect of elimination of a single site correlates with the efficiency of its glycosylation. We do not know whether each of the different N-glycosylated species of RAMP3 can reach the cell surface being assembled with CRLR. If this is the case, cell-surface expression of CRLR/RAMP3 receptors with different affinities to adrenomedullin could have some biological significance. Elimination of the six conserved cysteines results in the complete loss of receptor function but, surprisingly, only in a partial loss in the cell-surface expression of this mutant. A large difference in the expression levels could alter our measurement of EC_{50} by changing the ratio between wild-type or mutant receptors and their downstream effectors (G proteins). In the present study, the difference in cell-surface expression between CRLR/RAMP3 and CRLR/RAMP3-Δ4N and CRLR/RAMP3-Δ6C receptors is ∼2-fold (Figures 4C and 7B, respectively). To check whether this difference could be responsible for the decrease of AM potency to the CRLR/RAMP3-Δ4N mutant and the loss of function of the CRLR/RAMP3-Δ4N mutant, we performed the ligand binding analysis on oocytes expressing wild-type and mutant receptors. We show that the CRLR/RAMP3-Δ4N mutation results in a dramatic decrease in ^{125}I-AM affinity, and the CRLR/RAMP3-Δ6N mutation completely abolishes AM binding. These data suggest that a decrease or loss in AM affinity is mostly responsible for a decrease or loss of function of CRLR/RAMP3-Δ4N and CRLR/RAMP3-Δ6C mutants, respectively. Interestingly, one of the conserved cysteines (Cys^{56}) is the neighbor residue to the recently identified seven-residue segment that is responsible for adrenomedullin binding specificity (*4*, *5*). Whether disulfide bond formation is mostly required for the correct folding of this RAMP3 segment or other yet unidentified segments also involved in adrenomedullin binding remains to be established.

REFERENCES

1. McLatchie, L. M., Fraser, N. J., Main, M. J., Wise, A., Brown, J., Thompson, N., Solari, R., Lee, M. G., and Foord, S. M. (1998) *Nature 393*, 333−9.
2. Husmann, K., Sexton, P. M., Fischer, J. A., and Born, W. (2000) *Mol. Cell Endocrinol. 162*, 35−43.
3. Fraser, N. J., Wise, A., Brown, J., McLatchie, L. M., Main, M. J., and Foord, S. M. (1999) *Mol. Pharmacol. 55*, 1054−9.
4. Kuwasako, K., Kitamura, K., Ito, K., Uemura, T., Yanagita, Y., Kato, J., Sakata, T., and Eto, T. (2001) *J. Biol. Chem. 8*, 8.
5. Kuwasako, K., Kitamura, K., Onitsuka, H., Uemura, T., Nagoshi, Y., Kato, J., and Eto, T. (2002) *FEBS Lett. 519*, 113−6.
6. Sexton, P. M., Albiston, A., Morfis, M., and Tilakaratne, N. (2001) *Cell Signal 13*, 73−83.
7. Muff, R., Born, W., and Fischer, J. A. (2001) *Peptides 22*, 1765−72.
8. Flahaut, M., Rossier, B. C., and Firsov, D. (2002) *J. Biol. Chem. 277*, 14731−7.
9. Geering, K., Girardet, M., Bron, C., Kraehenbühl, J.-P., and Rossier, B. C. (1982) *J. Biol. Chem. 257*, 10338−43.
10. Chraibi, A., Schnizler, M., Clauss, W., and Horisberger, J. D. (2001) *J. Membr. Biol. 183*, 15−23.
11. Roitsch, T., and Lehle, L. (1989) *Eur. J. Biochem. 181*, 525−9.
12. Holst, B., Bruun, A. W., Kielland-Brandt, M. C., and Winther, J. R. (1996) *EMBO J. 15*, 3538−46.
13. McGinnes, L. W., and Morrison, T. G. (1997) *J. Virol. 71*, 3083−9.
14. Tanaka, K., Kitagawa, Y., and Kadowaki, T. (2002) *J. Biol. Chem. 277*, 12816−23.
15. Heerding, J. N., Hines, J., Fluharty, S. J., and Yee, D. K. (2001) *Biochemistry 40*, 8369−77.
16. Kono, M., Yu, H., and Oprian, D. D. (1998) *Biochemistry 37*, 1302−5.
17. Zhang, P., Johnson, P. S., Zollner, C., Wang, W., Wang, Z., Montes, A. E., Seidleck, B. K., Blaschak, C. J., and Surratt, C. K. (1999) *Brain Res. Mol Brain Res. 72*, 195−204.
18. Zhou, A. T., Assil, I., and Abou-Samra, A. B. (2000) *Biochemistry 39*, 6514−20.
19. Hawtin, S. R., Davies, A. R., Matthews, G., and Wheatley, M. (2001) *Biochem. J. 357*, 73−81.
20. Couvineau, A., Fabre, C., Gaudin, P., Maoret, J. J., and Laburthe, M. (1996) *Biochemistry 35*, 1745−52.
21. Muff, R., Buhlmann, N., Fischer, J. A., and Born, W. (1999) *Endocrinology 140*, 2924−7.
22. Christopoulos, G., Perry, K. J., Morfis, M., Tilakaratne, N., Gao, Y., Fraser, N. J., Main, M. J., Foord, S. M., and Sexton, P. M. (1999) *Mol. Pharmacol. 56*, 235−42.
23. Buhlmann, N., Aldecoa, A., Leuthauser, K., Gujer, R., Muff, R., Fischer, J. A., and Born, W. (2000) *FEBS Lett. 486*, 320−4.
24. Kamitani, S., and Sakata, T. (2001) *Biochim. Biophys. Acta 1539*, 131−9.
25. Robert-Nicoud, M., Flahaut, M., Elalouf, J. M., Nicod, M., Salinas, M., Bens, M., Doucet, A., Wincker, P., Artiguenave, F., Horisberger, J. D., Vandewalle, A., Rossier, B. C., and Firsov, D. (2001) *Proc. Natl. Acad. Sci. U.S.A. 98*, 2712−6.
26. Hanwell, D., Ishikawa, T., Saleki, R., and Rotin, D. (2002) *J. Biol. Chem. 277*, 9772−9.
27. De La Rosa, D. A., Li, H., and Canessa, C. M. (2002) *J. Gen. Physiol. 119*, 427−42.
28. Buller, A. L., and White, M. M. (1990) *J. Membr. Biol. 115*, 179−89.
29. Ghosh, S., Cox, K. H., and Cox, J. V. (1999) *Mol. Biol. Cell 10*, 455−69.
30. Riteau, B., Rouas-Freiss, N., Menier, C., Paul, P., Dausset, J., and Carosella, E. D. (2001) *J. Immunol. 166*, 5018−26.
31. Nicke, A., Baumert, H. G., Rettinger, J., Eichele, A., Lambrecht, G., Mutschler, E., and Schmalzing, G. (1998) *EMBO J. 17*, 3016−28.
32. Williams, R. T., Senior, P. V., Van Stekelenburg, L., Layton, J. E., Smith, P. J., and Dziadek, M. A. (2002) *Biochim. Biophys. Acta 1596*, 131−7.
33. Morelle, W., Haslam, S. M., Ziak, M., Roth, J., Morris, H. R., and Dell, A. (2000) *Glycobiology 10*, 295−304.
34. Hilairet, S., Foord, S. M., Marshall, F. H., and Bouvier, M. (2001) *J. Biol. Chem. 276*, 29575−81.
35. Kuwasako, K., Kitamura, K., Uemura, T., Nagoshi, Y., Kato, J., and Eto, T. (2003) *Hypertens Res. 26*, S25−31.
36. Nilsson, I. M., and von Heijne, G. (1993) *J. Biol. Chem. 268*, 5798−801.
37. Hasler, U., Greasley, P. J., von Heijne, G., and Geering, K. (2000) *J. Biol. Chem. 275*, 29011−22.
38. Gavel, Y., and von Heijne, G. (1990) *Protein Eng. 3*, 433−42.
39. Whitley, P., Nilsson, I. M., and von Heijne, G. (1996) *J. Biol. Chem. 271*, 6241−4.
40. Geetha-Habib, M., Park, H. R., and Lennarz, W. J. (1990) *J. Biol. Chem. 265*, 13655−60.
41. Jethmalani, S. M., Henle, K. J., and Kaushal, G. P. (1994) *J. Biol. Chem. 269*, 23603−9.
42. Kolhekar, A. S., Quon, A. S., Berard, C. A., Mains, R. E., and Eipper, B. A. (1998) *J. Biol. Chem. 273*, 23012−8.
43. Geering, K. (2001) *J. Bioenerg. Biomembr. 33*, 425−38.

BI0347508